A. Corazza
F. Vianello
L. Zennaro
N. Gourova
M.L. Di Paolo
L. Signor
O. Marin
A. Rigo
M. Scarpa

Enzyme mimics complexing Cu(II) ion: structure–function relationships

Authors' affiliations:
A. Corazza and M. Scarpa,
Department of Physics and INFM, University of Trento, Via Sommarive 14, 38050 Povo-Trento, Italy.

A. Corazza, F. Vianello, L. Zennaro, N. Gourova, M.L. Di Paolo, L. Signor, O. Marin and A. Rigo,
Department of Biological Chemistry, University of Padova, Via G. Colombo 3, 35100 Padova, Italy.

Correspondence to:
Dr *Marina Scarpa* PhD
Department of Physics
Via Sommarive 14
38050 Povo Trento
Italy
Tel: + 39 49 8276101; + 39 461 882029
Fax: + 39 49 8073310
E-mail: scarpa@science.unitn.it

Dates:
Received 8 January 1999
Revised 9 March 1999
Accepted 16 May 1999

To cite this article:
Corazza, A., Vianello, F., Zennaro, L., Gourova, N., Di Paolo, M.L., Signor, L., Marin, O., Rigo, A. & Scarpa, M. Enzyme mimics complexing Cu(II) ion: structure–function relationships.
J. Peptide Res., 1999, **54,** 491–504

ISSN 1397–002X

Key words: copper proteins; kinetics; mimics; molecular modeling; NMR; peptide design

Abstract: Five peptides containing (His-X_2)-His or (His-X_3)-His motifs have been designed and synthesized to coordinate Cu(II). Structural information was obtained by various spectroscopic techniques and was used as constraint to search for local conformational energy minima by molecular mechanics. Thermodynamic stability constants of the Cu(II) chelates was obtained by ^{19}F-NMR. The synthesized Cu(II)–peptide chelates were tested as catalysts of some important red-ox processes occuring in biological systems, in particular oxidation of ascorbate and dismutation of superoxide ion. The catalytic efficiency of the five chelates was much lower than that of ascorbate oxidase. On the contrary, two of them showed kinetic constants for superoxide dismutation about one order of magnitude lower than that of the enzyme Cu,Zn superoxide dismutase. In both cases, the catalytic properties were dependent on the peptide sequence. The relationships between structure and activity are discussed to find the structural parameters crucial for catalytic activity that can be modulated by appropriate design and synthesis of the peptides.

Much information on copper-containing proteins has become available during the last years. In particular composition and 3D structures have been obtained by biochemical and spectroscopic techniques and reactivity has been investigated to understand the biological function. In this regard, it appears that copper proteins can perform a large variety of biological functions. In fact, this class of proteins 'activates' oxygen allowing it to combine with carbon compounds (oxygenases) or hydrogen (oxidases) (1), or carry oxygen reversibly (hemocyanin) or act as electron

transferring compounds (plastocyanin) (2). The role of copper proteins in oxygen metabolism shows some peculiarities, since proteins acting as oxidases catalyze reactions generating highly reactive oxygen species that are enzyme-bound intermediates or released into the medium as harmful by-products. On the other hand the Cu,Zn superoxide dismutase protects cells from reactive oxygen species catalyzing the dismutation of the superoxide ion produced by one-electron reduction of molecular oxygen (3) and does not show any oxidase or oxygenase activity. A challenging goal is to understand why members of the copper protein family show such different behavior in the reaction pathways involving oxygen species. To reach this goal two aspects have to be investigated: the role of the protein matrix (the hydrophobicity, the electrostatic force field, the steric hindrance, etc.) and the importance of the structural arrangement of the copper site. Regarding the second point, in spite of the large number of studies on this subject, little is known about the relationships between the coordination sphere of the Cu(II) and its catalytic function. This lack of information notwithstanding the large amount of available data is mainly due to the complexity of copper protein architecture, which makes difficult a rational analysis of experimental data to correlate structure to reactivity. A possible approach to overcome this problem is to design and synthesize small compounds on the basis of a known enzyme structure, which should reproduce the arrangement of the functional groups of the active site. These compounds have been indicated as enzyme mimics (4, 5). In the case of the low molecular weight mimics of copper enzymes, it can be expected that the catalytic behavior of these copper complexes reflects the intrinsic properties of the coordination unit. It follows that knowledge of the relationships between structure and activity of these complexes permits the deduction of the minimal site structure needed to accomplish the biological function (6). Moreover the great advantage of the mimics is that their function can be modulated by systematic changes in their amino acid sequence. In this way, structural characteristics such as flexibility of the coordination site, polarity, hydrophobicity, can be easily correlated to reactivity. The mimics are also of interest for their possible technological applications since these artificial systems showing catalytic activity are easier to manipulate and are characterized by a longer lifetime with respect to proteins. Moreover, provided that some knowledge of the relationships between structure of the coordination unit and activity has been obtained, the functional properties of the artificial molecules should be changed by modification of some structural parameters, as required by the specific application.

In an attempt to find some of the relationships between structure of the copper coordination unit and biological function, we investigated model complexes between various oligopeptides and Cu(II).

These peptides were synthesized to create a binding site for the copper ion. A systematic study of the structure of the binding site and of the catalytic activity of these compounds in some biologically relevant reactions, that is the oxidation of ascorbate by molecular oxygen and the dismutation of superoxide ion, was performed as a function of the peptide sequence. The relationships between structure and catalytic properties were analyzed to identify the parameters that optimize the catalytic efficiency toward the ascorbic acid oxidation and superoxide ion dismutation.

Experimental Procedures

Materials

All chemicals were of the purest grade available.

The Boc-amino acids were purchased from Novabiochem (Läufelfingen, Switzerland). Ascorbate was from Fluka (Buchs, Switzerland). Catalase (H_2O_2: H_2O_2 oxidoreductase, E.C. 1.11.1.6), Cu,Zn superoxide dismutase (superoxide: superoxide oxidoreductase; E.C. 1.15.1.1), ascorbate oxidase (L-ascorbate: oxygen oxidoreductase, E.C. 1.10.3.3) imidazole and histidine were from Sigma (St. Louis, LO, USA).

The water used to prepare the solutions was twice-distilled and then passed through a Milli-Q purification system (Millipore, Bedford, MA, USA). To avoid heavy metal ion impurities, the glassware and the solutions were cleaned as already described (7).

Peptide synthesis

Peptide synthesis was performed by the solid-phase method/Fmoc strategy (8) on a preloaded Wang resin (Novabiochem) (0.1 mmol) using an automated peptide synthesizer (Applied Biosystem model 431A). Fmoc-protected amino acids were used with the following side chain protection: tert-butyl (tBu) for Ser, Glu and Asp; trityl (trt) for His; tert-butylcarbonyl (boc) for Lys; 2,2,5,7,8-pentamethyl-chromane-6-sulfonyl (Pmc) for Arg. The chain elongation was performed using 10-fold excess (1.0 mmol) of each Fmoc-amino acid, 2-(1H-benzotriazol-1-yl)1,1,3,3-tetramethyluronium hexafluorophosphate (HBTU) (0.5 mmol)

and 1-hydroxybenzotriazole (HOBt) (0.5 mmol) (9) in the presence of diisopropylethylamine (DIEA) (1.0 mmol). N-terminal acetylation was obtained by treating the peptide resin with 10% acetic anhydride in NMP. The peptides were cleaved from the resin and deprotected by treating with 95 : 3:1 : 1 (v : v) mixture of trifluoroacetic acid: anisole: 1,2-ethanedithiol: ethyl methyl sulfide, for 2 h. The crude peptides were purified either by ion exchange chromatography on CM Fast Flow resin (Pharmacia, Uppsala, Sweden) or by preparative reverse-phase HPLC on a C18 column (Delta Pak Water, Paris, France). The correct sequence of peptides was checked by mass analysis on a MALDI TOF spectrometer (Maldi 1/Kratos-Shimadzu) and the purity was $> 95\%$ by analytical HPLC. The peptides were stored as lyophilized powder at – 80°C and were dissolved in H_2O or H_2O/D_2O, or in the buffer, just before use. The pH or pH-pD of the solution was adjusted to 7.0. The peptide concentration in solution was checked by NMR, by comparison of the intensity of the resonance of the His residues of the peptides with that of free His under the same experimental conditions. Alternatively, when tryptophan was present in the peptide sequence, the peptide concentration was measured by optical absorption at 280 nm.

Preparation of complexes

Cu(II) and Zn(II) solutions were prepared by dissolving a small piece of Cu (purity > 99.8%) or Zn (purity > 99.99%) in 0.1 M HNO_3 and 0.1 M HCl, respectively.

The complexes were prepared by adding the metal ion to the peptide solution. The pH was adjusted to 7.0 after addition of the metal ion solution.

Spectroscopic studies

The ^{19}F-NMR relaxation parameters were measured with a pulse spectrometer operating at 16 MHz, using a Bruker Magnet and a home-built unit for pulse generation and detection. Acquisition and analysis were performed with a PC using a software developed in our laboratory which was written in Basic (Microsoft Quick Basic 4.5) on the basis of National Instruments standard libraries. The longitudinal relaxation time (T_1) was measured using the 90-τ-90 pulse sequence.

The paramagnetic contribution of Cu(II) complexes to the longitudinal relaxation rate $(T_{1P})^{-1}$, was calculated according to the relationship:

$$(T_{1P})^{-1} = (T_{1,obs})^{-1} - (T_{1,o})^{-1}$$

where $(T_{1,obs})^{-1}$ is the measured relaxation rate of the solution of the Cu(II) complex and $(T_{1,o})^{-1}$ is that of the peptide solution before Cu(II) addition.

^{1}H-NMR spectra were obtained on a Bruker MSL 300 spectrometer. High resolution 1D spectra were acquired by standard pulse microprograms. 2D TOCSY spectra (10) of the free peptides were acquired with a spectral width of 10 p.p.m., acquisition time 0.171 s, relaxation delay of 2 s. A spin-lock time (MLEV-17) of 60 ms was used with 1 K data points in t_2 dimension and 128 or 256 increments in t_1 dimension. This was zero filled to 2 k × 2 k. Two trim pulses of 2.5 ms were introduced at the beginning and at the end of the MLEV-17 sequence. The resonance assignments were accomplished on a manual basis (11). 3-(trimethylsilyl)propionic-2,2,3,3-d_4 acid (TMSP) was used as reference for chemical shift assignments.

X-band ESR spectra were obtained at 77 K on a Bruker ER 200D spectrometer. The optical spectra were obtained on a Perkin-Elmer Lambda 17 instrument.

Molecular modeling of copper complexes

We have performed a molecular mechanics geometry optimization on Cu(II)-peptides. A search for energy minima was conducted using the AMBER force field (12) and optimizing the geometry with a Steepest-descent algorithm for a first coarse optimization followed by a Polak-Ribière algorithm. The minimization ended when a RMS (root mean square) gradient of 0.1 kcal/(Åmol) was found. The program used was Hyperchem (Hypercube, Inc.) running on a PC Pentium.

Measurement of catalytic activity

The oxidation of ascorbic acid by molecular oxygen was followed by spectrophotometry, at 265 nm. The kinetic runs were carried out in 0.1 M potassium phosphate, pH 7.0, at 25°C. Usually 30 nM catalase was added to avoid possible side reactions due to H_2O_2 generated in the oxidation process. The ascorbate spontaneous oxidation was measured for each kinetic run, before the addition of the complex between polypeptides and Cu(II) and under our experimental conditions it was always < 0.1 nM/s. Solutions of known oxygen concentration were obtained by equilibration of the solutions with N_2–O_2 gas mixtures, in the PO_2 range 0–1 atm, at 25°C. Experimental details of the kinetic run performance have been previously reported (7).

The superoxide dismutase activity was measured at the Dropping Mercury Electrode (DME) by the polarographic

method of the catalytic currents (13) and by a method based on competition with cytochrome c (14). The polarographic measurements were performed in 0.1 M borate saturated with triphenylphosphine oxide, at pH 9.9, since the contribution of the spontaneous oxidation of superoxide is negligible at this pH value. A microcell (volume 800 μL) was used for polarographic measurements. The polarographic method of the catalytic currents is based on the monitoring of the one-electron reduction wave of molecular oxygen at increasing concentrations of the Cu(II)–peptide complex. Usually the concentration of the Cu(II)–peptide complex in these measurements was in the range 1–20 μM and the ratio [peptide]/[Cu(II)] was always > 15. The baseline of the one-electron reduction wave of molecular oxygen was recorded in the presence of 10 μM free peptide. Superoxide dismutase activity measurements were also performed at pH 7.0 and 9.9 as described by Fridovich (14).

An Amel 466 apparatus was used for polarographic measurements.

Results and Discussion

Peptide design

A preliminary study was performed to design polypeptides expected to show a binding site with high affinity for Cu(II). The starting points for polypeptide design can be summarized as follows:

- The peptides should contain some amino acid residues believed to be crucial for the binding of copper ions. The amino acids believed to participate in the binding were chosen on the basis of their metal ion binding strength (15), of the hard/soft classification (16) and of the active site structure of some copper proteins, involved in electron transfer reactions, such as superoxide dismutase (17), ascorbate oxidase (18), hemocyanin (19). On the basis of the reported copper coordination environments, we decided that the peptides should contain as possible binding amino acids, three histidines close in sequence, as found for example in astacin (20), while the fourth Cu(II) ligand should be a variable group of the polypeptide chain or the C- or N-terminal group. Cysteine was not included in the sequence, in order to avoid -SH oxidation during the experiments.
- The residues between the histidines were chosen to give flexibility to the peptide chain to permit the folding around the metal ion. Two arrangements have been followed to introduce the His residues, that is the $(His\text{-}X_2)_2$-His and $(His\text{-}X_3)_2$-His motif. In particular, the $His\text{-}X_3\text{-}His$ motif which forms a flexible region (21) is a part of the metal-binding sites of several natural metalloproteins including the 'zinc-finger' DNA-binding proteins (22) and it has been successfully incorporated into cytochrome c as a synthetic binding site for Cu(II) (23); moreover the $His\text{-}X_3\text{-}His\text{-}X_2\text{-}His$ cluster has been observed in the Alzheimer's β-amyloid peptide where it probably constitutes a high affinity metal binding site (24). The residues indicated as X were varied according to the criteria reported in the following paragraphs, but usually at least one Ala residue was included.
- Amino acids neutral or bearing positive or negative charge were included in the various sequences, to investigate the role of the electrostatic interactions (25, 26).
- Long–range interactions were not usually taken into account, since the peptides synthesized were too small to fold in the absence of Cu(II). In one case Glu^-, Lys^+ pairs, spaced four residues apart were added, to increase the probability of formation of an α-helix secondary structure (27).
- In two cases the N-terminal group has been acetylated to eliminate the positive charge of the $\alpha\text{-}NH_3^+$ group (28).

On this basis we synthesized the peptides listed in Table 1. In particular:

- peptide 1 contains three His in the sequence according to the motif $(His\text{-}X_2)_2$-His
- peptide 2 is similar to peptide 1, except that Lys and Asp were substituted by Trp and Leu
- peptide 3, 4 and 5 contain the motif $(His\text{-}X_3)_2$-His
- in peptide 3, an Ala residue was added to each of the two $(His\text{-}X_2)$ motifs of peptide 1
- peptide 4 is as peptide 3, but Ala-Gly-Ser has been substituted by the more hydrophilic Pro-Arg-Arg and the N-terminal group has been acetylated
- peptide 5 is as peptide 4 except that two Glu, Lys residues spaced by Ala residues, were included for helix formation.

Effect of metal binding on ^{1}H NMR spectra

^{1}H NMR spectra of peptide solutions were acquired before and after addition of Cu(II), in an attempt to obtain information on the amino acid residues whose spectral features are modified by the binding of this metal ion. The selective broadening of lines induced by Cu(II) ion was monitored to locate the binding sites. Since in some cases the information obtained from broadening experiments could be equivocal (29), optical and ESR spectra were also acquired and the contribution of Cu(II) to the longitudinal

Table 1. **Amino acid sequence of the synthesized polypeptides**

Peptide	Sequence	Estimated charge at pH 7.0*
Peptide 1	NH_2-Lys-His-Asp-Ala-His-Gly-Ser-His-Gly-COOH	+ 0.94
Peptide 2	NH2-Trp-His-Leu-Ala-His-Gly-Ser-His-Gly-COOH	+ 0.94
Peptide 3	NH2-Lys-His-Asp-Ala-Ala-His-Ala-Gly-Ser-His-Gly-COOH	+ 0.94
Peptide 4	CH3CONH-Lys-His-Asp-Ala-Ala-His-Pro-Arg-Arg-His-COOH	+ 1.94
Peptide 5	CH_3CONH-Ala-Glu-Ala-Ala-Ala-Lys-Glu-Ala-Ala-Ala-Lys-His-Asp-Ala-Ala-His-Pro-Arg-Arg-His-C OOH	+ 0.94

For the polypeptides design see the text. *The charge at pH 7.0 was calculated from the values of the ionization constants of the free amino acids (49).

relaxation time of $^{19}F^-$ nucleus was measured. In fact the fluoride ion was demonstrated to be a good probe of the Cu(II) present in enzyme active sites (30, 31).

The ^{1}H NMR spectra of the peptides were recorded, as described in the Experimental Procedures section (see Fig. 1A for peptide 3). The assignments were made on the basis of 2D TOCSY spectra and pH titrations (not shown). Cu(II) titrations were performed and an example of the spectrum obtained for peptide 3 at [Cu(II)]/[peptide] = 0.1 is reported in Fig. 1(B). The addition of Cu(II) changes the spectral characteristics and the relaxation rates inducing the progressive broadening of all NMR resonances (see Table 2 where we listed the residues showing remarkable broadening effects during the titration). In particular, a broadening effect was observed for the protons of the imidazole ring of the three His residues. The half-height linewidth ($\Delta\nu_{1/2}$) of the $H^{\varepsilon 1}$ up-field histidine of the five chelates showed a linear increase at increasing [Cu(II)]/[peptide] ratio. From the titration experiments we found that the broadening induced by Cu(II) to the $H^{\varepsilon 1}$ His resonance of peptide 5 is similar to

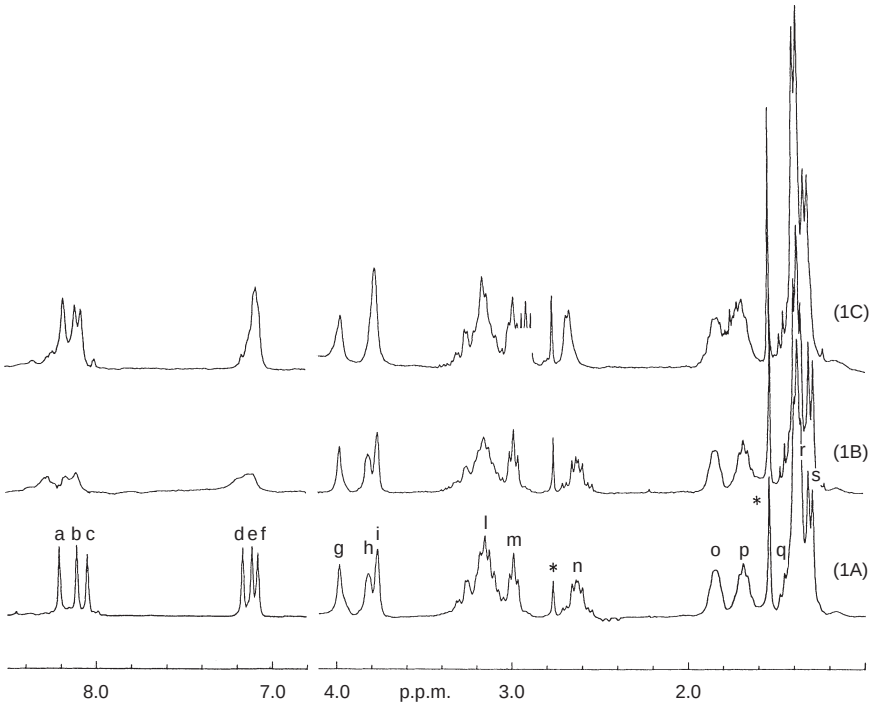

Figure 1. ^{1}H monodimensional NMR spectra of the peptide 3 at pH 7.0 (spectrum 1A) and upon complexation with 10% mol/mol Cu(II) and 100% mol/mol Zn(II) (spectrum 1B and 1C, respectively).(a, f) His $H^{\varepsilon 1}$, $H^{\delta 2}$ characterized by a pK_a = 6.5, respectively; (b, e) His $H^{\varepsilon 1}$, $H^{\delta 2}$ characterized by a pK_a = 6.9, respectively; (c, d) His $H^{\varepsilon 1}$, $H^{\delta 2}$ characterized by a pK_a = 7.2, respectively; (g) 8-Gly H^{α}; (h) 9-Ser H^{β}; (i) 11-Gly H^{α};(l) (2 + 6 + 10)-His H^{β}; (m) 1-Lys H^{ε}; (n) 3-Asp H^{β}; (o) 1-Lys H^{β}; (p) 1-Lys H^{δ}; (q) 1-Lys H^{γ}; (r) (5 + 7)-Ala H^{β}; (s) 4-Ala H^{β}; *) impurities. 1 mM peptide was dissolved in 0.1 M phosphate, pH 7.0. The solvent was 90% H_2O, 10% D_2O. Cu(II) or Zn(II) were added as a solution of 0.1 M Cu(II) in 1 M HNO_3 and 0.1 M Zn(II) in 1 M HCl, respectively. The spectra were acquired at 60° pulse width, 32 k spectrum size, 3 s repetition time, 128 scans. For the other experimental conditions, see text.

Table 2. **Peptide titrations with Cu(II) and Zn(II)**

	Cu(II) titration*	Zn(II) titration†
Peptide 1	$H^{\varepsilon 1}$, $H^{\delta 2}$ His 2, His 5 and His 8	- ‡
Peptide 2	$H^{\varepsilon 1}$, $H^{\delta 2}$ His 2, His 5 and His 8	- ‡
Peptide 3	$H^{\varepsilon 1}$, $H^{\delta 2}$ of His 2, His 6 and His 10	$H^{\varepsilon 1}$, $H^{\delta 2}$ His 2, His 6 and His 10; H^{β} Asp 3
Peptide 4	$H^{\varepsilon 1}$, $H^{\delta 2}$ His 2, His 6 and His 10	$H^{\varepsilon 1}$, $H^{\delta 2}$ His 2, His 6 and His 10; H^{β} Asp 3; H^{ε} Lys 1
Peptide 5	$H^{\varepsilon 1}$, $H^{\delta 2}$ His 12, His 16 and His 20	$H^{\varepsilon 1}$, $H^{\delta 2}$ His 12, His 16 and His 20; H^{β} Asp 13

In this table we reported the amino acids showing a remarkable modification of the spectral characteristics during the titration with Cu(II)* or Zn(II)†· H monodimensional NMR spectra of the peptides were acquired at pH 7.0 in 20 mM phosphate buffer in the presence of various concentrations of Zn(II) and Cu(II). Only the residues showing remarkable effects upon complexation were listed. *The half-height linewidth was taken as a significant spectral parameter. †The shift of the resonances was taken as a significant spectral parameter. ‡Not measurable.

that of peptide 4 (about 15–16 Hz at [Cu(II)]/[peptide](0.01) while this effect is weaker in the case of peptides 1–3 (about 1.5–2.5 Hz at [Cu(II)]/[peptide](0.01). From Fig. 1 it appears that the addition of Cu(II) also decreases the intensity of residues which do not participate directly to the binding of Cu(II). This effect can be explained on the basis of the strong paramagnetism of Cu(II) and assuming that Cu(II) is in fast exchange between the binding site and the bulk, according to the equilibrium:

$$\text{peptide} + \text{Cu(II)} \leftrightarrow \text{peptide} - \text{Cu(II)}$$

According to the relaxation theory (32), if fast exchange conditions hold, the plot of the logarithm of the paramagnetic contribution to the transversal relaxation rate, log $(T_{2P})^{-1}$, versus $(T)^{-1}$, where T is the absolute temperature, gave a straight line with negative slope (33). We acquired ^{1}H NMR spectra of solution of peptide 3 characterized by a ratio [Cu(II)]/[peptide] = 0.02, at various temperatures. The T_2 values of the histidines were measured from the half-height linewidth of the resonances. The $(T_{2P})^{-1}$, was calculated according to the relationship:

$$(T_{2P})^{-1} = [(T_{2,obs})^{-1} - (T_{2,o})^{-1}] \quad [1]$$

where $(T_{2,obs})^{-1}$ and $(T_{2,o})^{-1}$ are the T_2 values in the presence and the absence of Cu(II), respectively. Considering the $H^{\delta 2}$ histidine, whose resonance is at 7.11 p.p.m. from TMSP, in the range 280–320 K, we obtained the following relationship:

$$\log (T_{2P}) = -4.4 \times (T)^{-1} + 16.5 \quad [2]$$

which is in accord with the hypothesis of fast exchange. The presence of exchanging Cu(II) in the solution explains the broadening of the nonbonded resonances.

We attempted to overcome the loss of information due to the broadening of the NMR spectra of the Cu(II)–peptide systems, by preparing and characterizing the complexes of the five peptide-Zn(II). In fact, Zn(II) shows physicochemical characteristics similar to those of Cu(II). Zn(II) titrations were performed and the shift of the resonances of some amino acids, induced by the Zn(II), was taken as a significant marker of the binding. In Table 2 we report the resonances which are markedly shifted upon Zn(II) binding. On this basis, peptides 3, 4 and 5 appear to chelate the Zn(II), while peptides 1 and 2 show poor affinity toward this ion. In particular, since under these experimental conditions, that is at pH 7.0 and in the presence of 2 mM peptide, the formation of a precipitate following the addition of Zn(II) was observed, taking into account the solubility of Zn(II) at pH 7.0 (34), it was estimated that the binding constant between Zn(II) and the peptides 1 and 2 should be $< 10^4$ M^{-1}. The shift of the CH^{β}_2 resonance of the Asp as a function of the [Zn(II)]/[peptide] ratio was linear in the [Zn(II)]/[peptide] range 0–100%, according to the relationships:

CH^{β}_2 shift [p.p.m.] = 5.08×10^{-4} [Zn(II)]/[peptide]% + 2.624 for peptide 3

CH^{β}_2 shift [p.p.m.] = 4.66×10^{-4} [Zn(II)]/[peptide]% + 2.644 for peptide 4

CH^{β}_2 shift [p.p.m.] = 5.08×10^{-4} [Zn(II)]/[peptide]% + 2.668 for peptide 5.

^{19}F NMR relaxation rates

The strong broadening of the resonances of His residues of five peptides, due to Cu(II), results in a loss of structural information (such as NOE map). In contrast, information can be obtained by evaluating the paramagnetic contribution of Cu(II)–peptide chelates to the longitudinal relaxation rate $(T_{1P})^{-1}$, of suitable nuclear probes sensing the paramagnetic center. In fact the chemical exchange of a weak Cu(II) ligand (i.e. the nuclear probe) in large excess with

respect to the Cu(II) center, propagates the paramagnetic enhancement of the nuclear relaxation rate of the bound nuclei to the nuclei in the bulk solution. We decided to use the $^{19}F^-$ ion as a nuclear probe of the Cu(II) ion (30–32). The primary structure of the five peptides reported in Table 1 suggests that each of them may bind Cu(II) in a different way. In particular the possible presence of simultaneously existing species in the Cu(II)–peptide system should be taken into account when [Cu(II)]/[peptide] > 1. Assuming that *n* species, simultaneously existing in the solution contain Cu(II), the (T_{1P}) of the nuclear probe depends on the concentration of the copper species according to the relationship:

$$(T_{1P})^{-1} = \sum_{i=1}^{n} R_{iP}[L - Cu(II)]_i \qquad [3]$$

where $[L - Cu(II)]_i$ is the concentration and R_{iP} the molar relaxivity (M^{-1} s^{-1}) of the *i*th Cu(II)-containing species, respectively (35).

To investigate the presence of these species, we measured the (T_{1P}) of the five peptides listed in Table 1 as a function of the [Cu(II)]/[peptide] ratio (see Fig. 2). From Fig. 2 there appears a linear increase of (T_{1P}) at increasing Cu(II) concentration, up to [Cu(II)]/[peptide] $\approx$ 1 followed by a change of the slope at [Cu(II)]/[peptide] $\geq$ 1. The experimental data were fitted to eqn 3, by substituting the term [L – Cu(II)] on the basis of the chemical equilibria and the mass balances and assuming that at the maximum, two different Cu(II)–peptide complexes are present at [Cu(II)]/[peptide] $\leq$ 1.5 (see Fig. 2). The floating parameters were the ratio between the thermodynamic stability constants (K_1/K_2), and the relaxivities (R_{1P} and R_{2P}) of the two complexes. The fitting was satisfactory provided that $K_1 \gg K_2$, indicating that one copper species is predominant at [Cu(II)]/[peptide] $\leq$ 1. This species should be a chelate characterized by a [Cu(II)]/[peptide] ratio of 1 and by a stability constant higher than those of the other possible complexes. At [Cu(II)]/[peptide] $\geq$ 1 more copper complexes should be present. From Fig. 2 it appears also that the 1/1 complexes between Cu(II) and peptides 1–3 show similar molar relaxivity values (of the order of 10^5 M^{-1} s^{-1}), while the relaxivity values of the complexes between Cu(II) and peptides 4 and 5 are about one order of magnitude higher (see also Table 4 where the R_P values are listed).

Optical and ESR spectra

Electron-absorption and X-Band ESR spectra have been acquired for probing the structure of the various Cu(II) complexes (see Fig. 3). The data obtained from these spectra are summarized in Table 3 together with the spectroscopic characteristics of the complexes of Cu(II) with ethylendiaminetetracetic acid (Cu(II)–EDTA) and with histidine (Cu(II)–$(His)_2$).

Optical spectra have been acquired in the region between 300 and 800 nm and have been characterized in terms of wavelength and intensity of absorption bands of the most intense transitions in the visible region (see Table 3). Brill *et al*. (36) suggested that when oxygen atoms are replaced by nitrogen atoms in the first coordination sphere of Cu(II) ion, the wavelength maximum (λ_{max}) shifts to a shorter wavelength and the extinction coefficient usually increases. In particular crystal structure analysis and studies performed at pH values close to 7 have shown that one molecule of EDTA chelates the Cu(II) by two nitrogen atoms and four carboxylate oxygen atoms (37) while in the case of Cu(II)–$(His)_2$ two terdentate histidine anions chelate the Cu(II) by either imidazole and amino nitrogen and carboxylate oxygen atoms (15, 38). The absorption maxima for these two complexes are in agreement with the proposed structure since λ_{max} shifts from 735 nm for the Cu(II)–EDTA to 641 nm for Cu–$(His)_2$. On this basis the copper ion appears chelated by peptides 1–3 mainly by N ligands while N and O ligands should be involved in the Cu(II) binding by peptides 4 and 5.

The X band ESR spectra of the Cu(II) complexes have been acquired at 77 K, the Landé g factor and the hyperfine splitting constant A have been calculated and their values are reported in Table 3. To identify the donor atoms, a comparison between the ESR parameters reported in Table 3

Table 3. **Optical and magnetic parameters of Cu(II)–peptide chelates**

Cu(II) complex	λ_{max} (nm)	$\varepsilon_{\lambda max}$ (M^{-1} cm^{-1})	g_{II}	A_{II} (gauss)
Cu(II)-$(Histidine)_2$*	641	45	2.250	182
Cu(II)-EDTA†	735	78	2.348	135
Cu(II)-peptide 1‡	567	67	2.226	195
Cu(II)-peptide 2‡	557	63	2.195	211
Cu(II)-peptide 3‡	578	53	2.403	120
Cu(II)-peptide 4‡	702	27	2.413	117
Cu(II)-peptide 5‡	686	28	2.398	123

Optical and ESR spectra were recorded in 20 mM phosphate buffer at pH 7.0. The instrumental ESR settings were as in Fig. 5. *The complex stoichiometry was taken from Kruck and Sarkar (50); the spectra were acquired at 1 mM Cu(II), 2 mM histidine. †The spectra were acquired at 1 mM Cu(II), 1 mM EDTA. ‡The concentration of the complexes was about 1 mM for the optical experiments and, as reported in Fig. 5, for the ESR experiments. In all the experiments equimolar concentrations of Cu(II) and peptides were present.

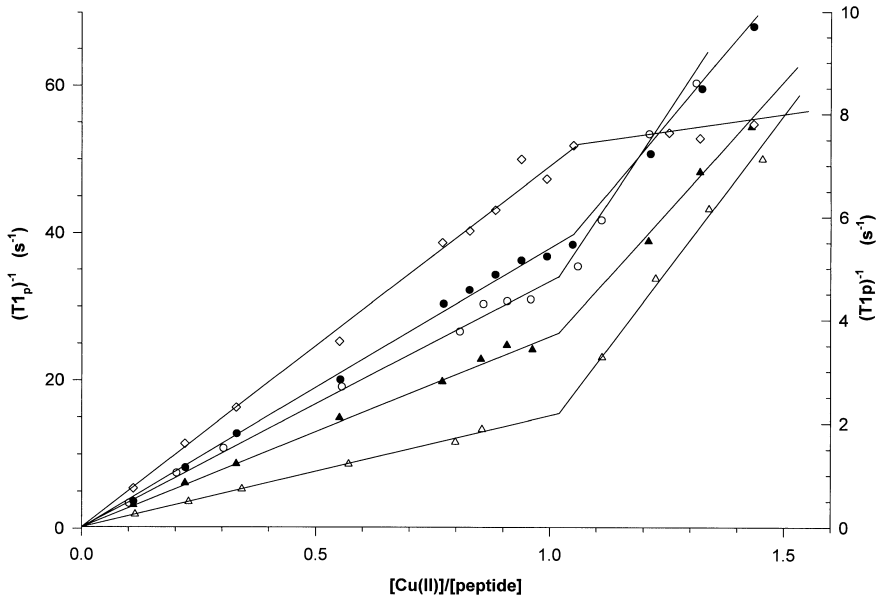

Figure 2 Dependence of the (T_{1P}) of the F^- on the [Cu(II)]/[peptide] ratio. The solution contained: 22 μM peptide 1 (○), 30 μM peptide 2 (▲), 30 μM peptide 3 (△), 15 μM peptide 4 (●), 50 μM peptide 5 (◇) in 50 mM Hepes, 0.5 M F^-, pH 7.0. The titration was performed by adding the desired amount of 0.1 mM Cu(II) in 1 mM HNO_3. The T_1 values were measured at 16 MHz as described in the Experimental Procedures. The solid lines were obtained by fitting the experimental data to eqn 3 assuming $n = 2$. The fitting was characterized by a ratio $MS_{reg}/MS_{res} > 2000$, where Ms_{reg} = regression variation from the dependent variable and Ms_{res} = residual variation.

with those reported in the Peisach–Blumberg plot (39) has been performed. According to this plot, g-values increase while the A values decrease as O replace N donor atoms and the regions of compounds O ligated, N ligated, and with different ligand coordination are set off. The comparison between the data of Table 3 and the Peisach–Blumberg plot further supports the coordination of Cu(II) by N donor atoms in peptides 1–2 and by N and O donor atoms in peptides 3–5, respectively. Among the N donor atoms the nitrogen of the imidazole ring appears the more favorite coordinating group, as shown by the broadening of ^{1}H NMR spectra (see Table 2). This datum is also in accord with the findings of Aiba *et al*. (40) who observed that small peptides such as Gly-His bind to Cu(II) through the imidazole nitrogen atoms. A fourth nitrogen atom can be provided by the N-terminal residue but an involvement of cupric ion interaction with peptide nitrogen atom cannot be excluded.

It appears likely that the O donor atoms in peptide 3–5 could be provided by Asp residue which is markedly shifted upon Zn(II) titration. However, Asp residue resonances are not selectively broadened at [Cu(II)]/[peptide] < 10% and an involvement of a water or a terminal carboxylic O could be hypothesized in the Cu(II) coordination.

Modeling the structure of Cu(II)–peptide complexes

The 3D structure of Cu(II)–peptide complexes was proposed following a molecular mechanics study based on AMBER

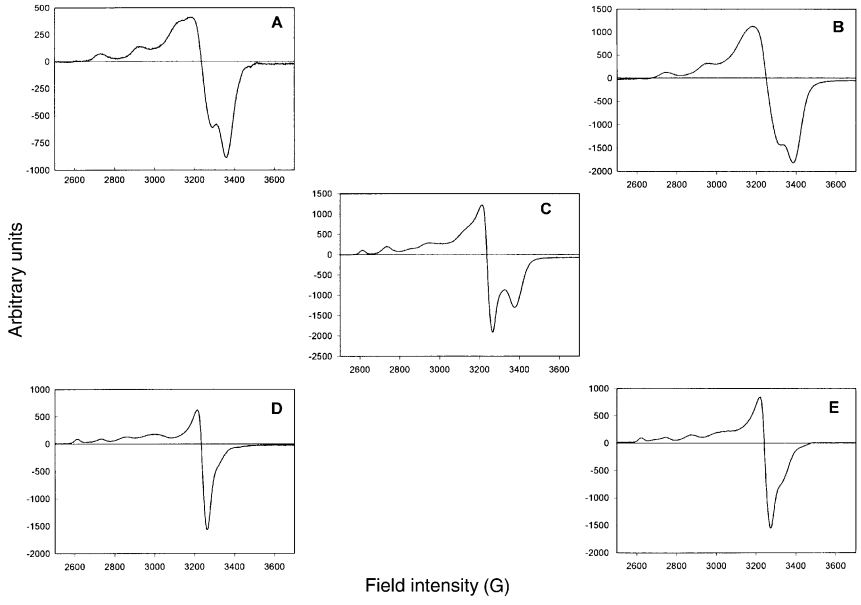

Figure 3. ESR spectra of Cu(II)–peptide complexes. The spectra were obtained at 77 K, 9.42 GHz, in 20 mM phosphate, pH 7.0, modulation frequency 100 KHz, scan width 1000 G, scan time 500 s, time constant 2 s, microwave power 20 mW. (A) 0.5 mM Cu(II)–peptide 1; (B) 1.6 mM Cu(II)–peptide 2; (C) 1.9 mM Cu(II)–peptide 3; (D) 1.8 mM Cu(II)–peptide 4; (E) 2.6 mM Cu(II)–peptide 5.

Table 4. **Thermodynamic stability constants of the complexes between peptides and Cu(II)**

Peptide	Competitor ligand*	K_P† (M^{-1})	R_P† (M^{-1} s^{-1})
Peptide 1	EDTA	$4.3 \pm 2.5 \times 10^{13}$	2.1×10^5
Peptide 2	EDTA	$1.6 \pm 0.1 \times 10^{14}$	1.4×10^5
Peptide 3	EDTA	$2.3 \pm 1.1 \times 10^{10}$	0.7×10^5
Peptide 4	Maleate	$1.4 \pm 0.5 \times 10^7$	2.4×10^6
Peptide 5	Maleate	$1.6 \pm 1.3 \times 10^8$	9.2×10^5

The thermodynamic stability constants of the peptide–Cu(II) complexes (K_P) were calculated by measuring the $(T_{1P})^{-1}$ of a solution containing the competitor ligand and Cu(II) at increasing peptide concentration. The measurements were performed in 50 mM Hepes containing 0.5 M KF, pH 7.0; peptides 1, 2, 3: 30 μM Cu(II), 30 μM EDTA, peptide 1, 2, or 3 were varied in the range 10–400 μM; peptide 4 and 5: 7 μM Cu(II), 100 mM maleate, peptide 4 or 5 were varied in the range 10–300 μM. *The values of the stability constants (K_C) reported in the literature were $K_C = 3.16 \times 10^{15}$ M for Cu(II)–EDTA and $K_C = 7.94 \times 10^{13}$ M^{-1} for Cu(II)–maleate. †R_P values as calculated from the $(T_{1P})^{-1}$ of 1 μM peptide–Cu(II) complex in 50 mM Hepes, pH 7.0, containing 0.5 M KF. R_C values calculated from the $(T_{1P})^{-1}$ of 1 μM ligand–Cu(II) complex in 50 mM Hepes, pH 7.0, containing 0.5 M KF were 1.8×10^4 M^{-1} s^{-1} and 4.6×10^5 M^{-1} s^{-1} for EDTA–Cu(II) and maleate–Cu(II) complexes, respectively.

Table 5. **Initial reaction rates (v_0) of the ascorbate oxidation in the presence of the Cu(II)-peptide complexes**

Cu(II)–complex	$v_0 \times 10^8$ (M s^{-1})
–*	< 0.01
Cu(II)–peptide 1	1.3
Cu(II)–peptide 2	2.0
Cu(II)–peptide 3	6.2
Cu(II)–peptide 4	13.0
Cu(II)–peptide 5	17.1
Cu(II)†	1.9
Ascorbate oxidase‡	7500

The initial reaction rates of the ascorbate oxidation (v_0) were measured in 0.1 M potassium phosphate, at pH 7.0 and 25°C in the presence of 30 nM catalase. The assay solution contained 0.6 mM ascorbate, 0.24 mM O_2 and 3 μM Cu(II); the peptide was in large excess with respect to the Cu(II), that is [peptide]/[Cu(II)] ≥ 15. *No addition of Cu(II). †Cu(II) ion was added as $Cu(II)(NO_3)_2$ in the absence of copper chelating species. ‡The experimental v_0 was measured in the presence of 5 nM Cu coordinated to ascorbate oxidase; the reported value was extrapolated to 3 μM coordinated copper ion, assuming a linear dependence of v_0 on ascorbate oxidase concentration.

force field (12). AMBER force field lacks of all the parameters related to the copper atom. The necessary parameters were obtained from the literature (41, 42). To model the copper binding site we followed a bonded approach based on spectroscopic data of copper ligands obtained from ESR, optical and NMR measurements on the Cu(II)–peptide complexes. Energy minimization produced for Cu(II)–peptide 1–5 complexes a tetrahedral geometry for the copper coordination site (see Fig. 4 where the projections of the structure of the complexes are reported). Peptides 1 and 2 bind the copper atom with Nε of the three His residues and with the N-terminal of Lys and Trp, respectively. Peptides 3–5 coordinate Cu with the Nε of the three His residues and with the carboxyl group of Asp. From the 3D structures it can be seen that the copper atom in peptide 4 and 5 complexes is more exposed to the solvent and a fifth bipyramidal coordination of a water molecule is plausible. Moreover peptide 5 forms a helix as expected from the planned sequence.

Thermodynamic stability constants of the Cu(II)–peptide complexes

The thermodynamic stability constants of the various Cu(II)–peptide complexes were estimated by allowing the peptide to compete for Cu(II) with a ligand having a known binding constant. The paramagnetic enhancement of the longitudinal relaxation rate of the $^{19}F^-$ ion was measured to monitor the equilibrium between Cu(II), the peptide (P) and the competitor ligand (C). We measured the $(T_{1P})^{-1}$ of solutions containing the Cu(II)–peptide-ligand system as a function of the [ligand]/[peptide] ratio at constant Cu(II) concentration and, under the condition:

$$[Cu]_o < [C] + [P]$$

where $[Cu]_o$ is the concentration of the added Cu(II). The molar relaxivity (R_M) of Cu(II) was calculated, that is:

$$R_M = \frac{(T_{1P})^{-1}}{[Cu]_0} \quad [4]$$

According to eqn 3 and assuming as previously reported that the Cu(II) forms one predominant chelate with the peptide (P-Cu(II)) and one with the competitor ligand (C-Cu(II)), the R_M of the system is given by the following relationship:

$$R_M = R_P x_P + R_C x_C \quad [5]$$

where R_p, R_C are the molar relaxivities and x_p, x_C are the molar fractions of the P–Cu(II) and C–Cu(II) chelates,

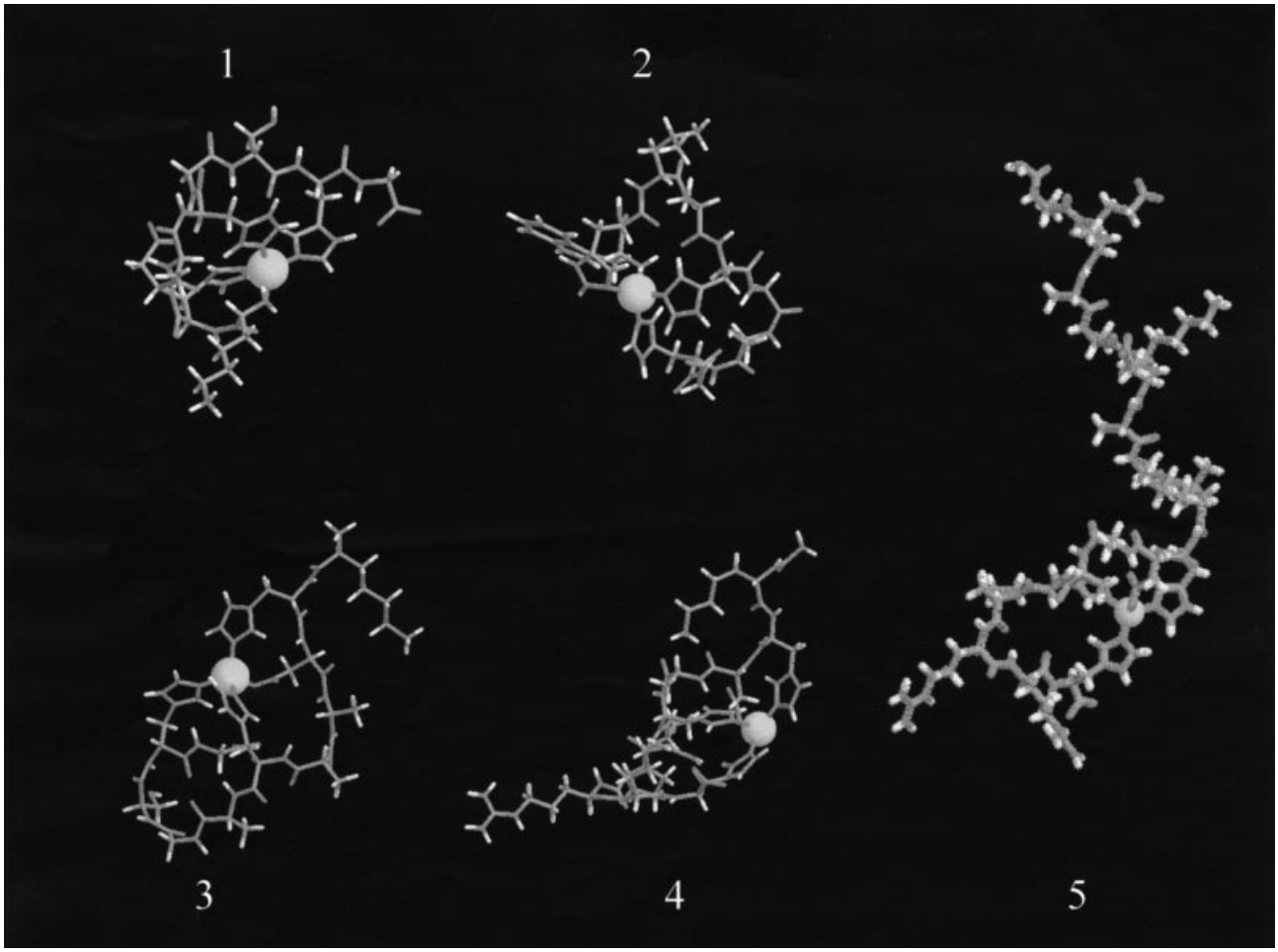

Figure 4. Proposed molecular structure of the Cu(II)–peptide complexes. The models were obtained by introducing the structural data into a molecular mechanic simulation program as described in the text. (1) Cu(II)–peptide 1 complex. The ligands are: Nε of His 2, His 5, His 8 and the N-terminal of Lys; (2) Cu(II)–peptide 2 complex. The ligands are: Nε of His 2, His 5, His 8 and the N-terminal of Trp; (3) Cu(II)–peptide 3 complex. The ligands are: Nε of His 2, His 6, His 10 and the carboxyl group of Asp; (4) Cu(II)–peptide 4 complex. The ligands are: Nε of His 2, His 6, His 10 and the carboxyl group of Asp; (5) Cu(II)–peptide 5 complex. The ligands are: Nε of His 2, His 6, His 10 and the carboxyl group of Asp.

respectively. Introducing the stability constant of C–Cu(II) and that of P–Cu(II), that is:

$$K_C = \frac{[C - Cu(II)]}{[C][Cu(II)]} \text{ and } K_p = \frac{[P - Cu(II)]}{[P][Cu(II)]},$$

into eqn 5 we obtain:

$$R_M = R_L - \frac{\frac{(R_C - R_P)}{[Cu]_0}}{2 \times \left(\frac{K_P}{K_C} - 1\right)} \times \left\{ [C]_0 - [Cu]_0 + ([Cu]_0 + [C]) \times \frac{K_P}{K_C} - \left\{ \left([C]_0 - [Cu]_0 + ([Cu]_0 + [P]) \times \frac{K_P}{K_C} \right)^2 - 4 \times \left(\left(\frac{K_P}{K_C} \right) - 1 \right) \times [Cu]_0 \times [P] \times \frac{K_P}{K_C} \right\}^{1/2} \right\} \quad [6]$$

where $[Cu]_o$ and $[C]_o$ are the total concentration of the Cu(II) and of the competitor ligand, [Cu(II)] is the concentration of the free Cu(II), [P] and [C] are the concentrations of the unbound peptide and of the free competitor ligand, respectively. The ligands used as peptide competitors were chosen on the basis of their R_C and K_C values. In particular we chose competitors with an R_C value about one order of magnitude lower than R_P and with K_C values comparable to K_P. To this regard preliminary competition trials were performed utilizing various Cu(II) ligands. On the basis of the results obtained, we used EDTA in the case of peptides 1–3 and maleate ion in the case of peptides 4 and 5.

The competition experiments were performed for each peptide measuring the R_M values of solutions at constant $[Cu]_o$, $[C]_o$ and variable $[P]_o$. The R_P and R_C values were calculated from (T_{1P}) of solutions containing the complexes P–Cu(II) and C–Cu(II), respectively. This set of experimental data, in addition to K_C, was used to fit eqn 6, with K_P as a parameter. The results obtained are summarized in Table 4. From this table it appears that the peptides are characterized

by high K_P values, as expected on the basis of the criteria followed for peptide design. Moreover the R_P values (in particular for peptides 4 and 5) are higher than those of many low molecular weight Cu(II) complexes and close to that of the Cu,Zn superoxide dismutase (30).

Ascorbate oxidation catalyzed by various Cu(II)–peptide chelates

The complexes between Cu(II) and the peptides listed in Table 1 were tested as catalysts of ascorbate oxidation by molecular oxygen.

The ascorbate oxidation rates (v_o) were measured in the presence of 3 μM Cu(II)–peptide chelate (see Experimental Procedures) and are reported in Table 5. In this table we reported also the v_o values obtained when a $Cu(NO_3)_2$ solution was added to the reaction medium in the absence of peptides, to obtain a 3-μM Cu(II) concentration. Under these conditions the Cu(II) present in solution is slightly bound to water molecules and to nitrate, phosphate ion or to ascorbate itself, the latter compound being a weak complexing agent at pH 7 (43). The five Cu(II)–peptide chelates induced a significant increase of the oxidation rate of ascorbate (under our experimental conditions the spontaneous oxidation in the absence of the metal complex was < 0.1 nM s^{-1}). However, the activity of the Cu(II)–peptide chelates was small in comparison to that of the enzyme ascorbate oxidase measured under the same experimental conditions.

We investigated the possibility that the electron transfer between ascorbate and oxygen occurs by a series of one-electron steps and the intermediate reaction products are released into the solution. To this regard we tested the involvement of superoxide ion in the ascorbate oxidation and ESR spectra searching for the ascorbyl radical ($A^{-\circ}$) resonance were recorded. In particular the rate of ascorbate oxidation catalyzed by the five Cu(II)–peptide complexes in the presence and in the absence of 5 μM Cu,Zn superoxide dismutase was recorded and it was observed that this enzyme reduced the ascorbate oxidation rate catalyzed by the various copper chelates by about 50%. A similar effect of Cu,Zn superoxide dismutase in the oxidation of ascorbate by molecular oxygen, catalyzed by Cu(II)-$(His)_2$ or by Fe(III)-EDTA was found. This effect was proposed to demonstrate a reaction mechanism where superoxide ion ($O_2^{-\circ}$) is generated and acts as an active reaction product since it reacts with ascorbate itself or with ascorbyl radical (44). Moreover the ESR spectrum of 0.5 mM ascorbate, in the presence of 0.25 mM oxygen and 5 μM Cu(II)–peptide in 0.1 M potassium phosphate at pH 7.0 was recorded and the characteristic resonance of the ascorbyl radical was observed (45). These results demonstrate that both the oxidation of ascorbate and the oxygen reduction catalyzed by the five Cu–polypeptide complexes occur through one-electron steps and the products $A^{-\circ}$ and $O2^{-\circ}$ are released into the solution. Also the oxidation of ascorbate catalyzed by ascorbate oxidase occurs through one-electron steps, as in the case of Cu(II)–peptides, where the ascorbyl radical is the intermediate reaction product. However, in the case of the enzyme, oxygen reactive species are not released into the solution since molecular oxygen is reduced directly to water. This behavior is due to the involvement of more than one copper ion of the enzyme in the electron transfer from ascorbate to molecular oxygen.

Lineweaver–Burk plots of experiments carried out at various oxygen or ascorbate concentrations showed a saturation of the reaction rate by these two substrates indicating that in spite of the quite low oxidase-like catalytic activity, the Cu(II)–peptide chelates behave like an enzyme and suggest that future modifications of the peptide sequence will improve the activity of the chelates as catalysts of the ascorbate oxidation.

Superoxide ion dismutation catalyzed by Cu(II)–peptides

The activity of the Cu(II)–peptides as catalysts of superoxide dismutation was tested by a method based on the inhibition of the cytochrome c reduction by superoxide ion (at pH 7.0 and 9.9) (14), and by the polarographic method of the catalytic currents (at pH 9.9) (13). The data obtained by the two methods indicated that the Cu(II)–peptide chelates are characterized by a superoxide dismutase activity. In particular we calculated the kinetic rate constant (k_d) of the overall superoxide dismutation reaction catalyzed by the various Cu(II)–peptides that have been synthesized in this laboratory and the k_d values obtained are reported in Table 6. From this table there appears to be good agreement between the values obtained by the polarographic method (13) and cytochrome c method (14) which permits the calculation of the absolute and relative values of k_d, respectively.

Furthermore it appears that the five Cu(II)–peptide chelates have a remarkable dismutase-like activity which in the case of peptide 4 is about 1/50 than that of Cu,Zn superoxide dismutase. This indicates that the designed Cu(II)–peptide chelates behave much more like superoxide dismutase than ascorbate oxidase. High superoxide dismutase activity of low molecular weight complexes between Cu(II) and histidine-containing oligopeptides was observed by other authors (46–48). However, the peptides studied by

Table 6. **Kinetic constants for superoxide dismutation observed in the presence of the Cu(II)–peptide complexes**

	$k_d \times 10^6$* (M^{-1} s^{-1})		
Cu(II)–complex	**pH 7.0†**	**pH 9.9‡**	**pH 9.9§**
Cu(II)–peptide 1	0.70	0.10	0.17
Cu(II)–peptide 2	0.15	0.12	0.14
Cu(II)–peptide 3	0.06	0.05	0.10
Cu(II)–peptide 4	38.00	1.10	1.08
Cu(II)–peptide 5	11.00	1.30	1.30
Cu(II)¶	–	–	–

*Kinetic rate constant for superoxide dismutation.
†Measured from inhibition of the cytochrome c reduction. The solution contained: 0.1 M phosphate, pH 7.0, 0.03 μM catalase, 0.5 mM xanthine, 50 μM Fe(III)-cytochrome c. The superoxide generation was started by the addition of xanthine oxidase and was of the order of 0.02 μM s^{-1}. The k_d values were calculated assuming that the kinetic rate constant of Fe(III)-cytochrome c reduction by superoxide is 1.4×10^6 M^{-1} s^{-1} at pH 7 and 0.9×10^5 M^{-1}·s^{-1} at pH 10 (51).
‡As † except that the buffer was 0.10 M borate pH 9.9; the measurements were run in triplicate and the standard deviation was < 8%.

these authors contained two to four amino acids among which Gly residues were present and did not simulate copper-enzymes binding sites.

Relationships between structure and catalytic activity

The possible relationships between the structure of the copper environment, which had been varied on the basis of the rational approach that was reported previously, and the catalytic activity were investigated. From an analysis of the spectroscopic information, the stability constants and activity data, it appears that the peptides of Table 1 can be divided into two groups:

- Peptides 1 and 2 which coordinate the Cu(II) mainly by nitrogen atoms. These peptides form complexes with Cu(II) characterized by a high stability constant (of the order of 10^{14} M^{-1}), by a relatively weak linebroadening effect on ^1H resonances of noncoordinating residues and by a molar relaxivity with respect to $^{19}F^-$ of the order of 10^5 M^{-1} s^{-1}. Furthermore these peptides do not coordinate the Zn(II).
- Peptide 4 and 5 coordinate Cu(II) by nitrogen and oxygen atoms and also coordinate Zn(II). These Cu(II)–peptide complexes are characterized by stability constants of the order of 10^7–10^8 M^{-1} and by a very high molar relaxivity (of the order of 10^6 M^{-1} s^{-1}). They also show a strong linebroadening effect on ^1H resonances of noncoordinating residues.

From the data of Tables 5 and 6 it appears that the two groups are also distinguishable on the basis of their catalytic activity. In fact from the data of Tables 5 and 6, the second group shows the highest ascorbate oxidase- and superoxide dismutase-like activity.

These characteristics can be explained from the molecular structure shown in Fig. 4. In fact, in the complexes of peptide 4 and 5, the $(His\text{-}X_3)_2$-His motif gives flexibility to the polypeptide chain which folds leaving the Cu(II) site opened from one side, whereas Cu(II) in the complexes of peptide 1 and 2 is less accessible. The accessibility of Cu(II) to weak copper ligands such as fluoride ion, and substrates such as ascorbate or superoxide, can explain the relatively high values of the relaxivity of $^{19}F^-$ and of the catalytic activity that has been measured. In fact, it appears that access to Cu(II), rather than the charge around the copper coordination environment, is responsible for the different behavior of the two groups of Cu(II) complexes. However, a contribution of the surface charge is indicated from the dismutase-like activity data, since the k_d values obtained at pH 7.0 and 9.9 of the Cu(II)–peptide complexes containing amino acid residues bearing NH_3^+ groups in the peptide sequence, decrease at alkaline pH values (see peptides 1, 4 and 5). This indicates that the electrostatic interaction between the positive charges and superoxide facilitates the catalytic event. However, the effect of pH on k_d values could be partially due to the modification of the coordination geometry of the complexes. An indication of the effect of the positive charge-bearing residues is indicated by the superoxide dismutation and the ascorbate oxidation rates when the sequence of the three neutral spacers Ala-Gly-Ser was substituted by Pro-Arg-Arg bearing a 2+ charge (compare Cu(II)–peptide 3 with Cu(II)–peptide 4). This increase was retained after the addition to the backbone of peptide 4 of an oligopeptide, which contains four Ala residues and two couples (Glu^--Lys^+), capable of helix stabilization by salt bridges (compare Cu(II)–peptide 4 with Cu(II)–peptide 5).

Peptide 3 shows anomalous behavior since some features of the Cu(II)–peptide 3 complex are similar to those of the first family (optical characteristics, and linebroadening effect), and other features are similar to those of the second family (ESR parameters, involvement of Asp residue in the metal coordination, coordination of Zn(II)). This behavior can be explained since the sequence of peptide 3 is similar to that of peptide 1 (apart from two Ala residues required to create the $(His\text{-}X_3)$-His motif).

In previous studies performed on superoxide dismutase a good correlation between the dismutase-like activity and

the paramagnetic contribution to the F^- relaxation rate (R_P) (30) was observed, since F^- behaves as a superoxide ion (25). To this regard, the plot of the experimental molar relaxivity of the Cu(II)–peptide complexes (see the R_P values reported in Table 4) versus their k_d values at pH 7 (see Table 7) is fitted by the linear equation: $R_P = 6.02 \times 10^{-2}\ k_d + 1.57$ ($r = 0.996$). This linear relationship indicates the strong correlation between the catalytic properties and the spectroscopic characteristics, which, in turn, are dependent on the active site structure.

In conclusion, notwithstanding that the results obtained up to now do not permit general conclusions on the structure–function relationships in small peptides chelating the Cu(II) to be drawn, they do permit the conclusion that some structural aspects are crucial for the catalytic activity of the synthesized peptides. In particular: both the $(His\text{-}X_2)_2$-His and $(His\text{-}X_3)_2$-His motifs permit flexibility in the peptide coordination structure around the Cu(II) ion, but the stability constants of the $(His\text{-}X_2)_2$-His motif are about 5–6 orders of magnitude higher. In contrast, only the $His\text{-}X_3$-His motif is suitable for Zn(II) coordination.

The paramagnetic contribution of the five Cu(II)–peptide complexes to the F^- relaxation rate is very high if compared to that of the majority of low molecular weight Cu(II) complexes and close to that of the enzyme Cu,Zn superoxide dismutase. In particular the molar relaxivity of the Cu(II)–peptide 4 complex is the highest and is in accord with the electrostatic field induced by the high positive charge of this peptide (+ 1.94 at pH 7).

References

1. Hayaishi, O. (1974) General properties and biological functions of oxygenases. In *Molecular Mechanism of Oxygen Activation* (Hayaishi, O., ed.). Academic Press, New York pp. 1–28.
2. Sykes, A.G. (1991) Plastocyanin and the blu copper proteins. In *Long Range Electron Transfer in Biology. Structure and Bonding* 75 (Clarke M.J., Goodenough, J.B., Jørgensen C.K., *et al.*, eds). Springer-Verlag, Berlin, pp. 175–224.
3. Fridovich, I. (1972) Superoxide radical and superoxide dismutase. *Acc. Chem. Res.* **5**, 321–326.
4. De Grado, W.F. (1989) Design of peptides and proteins. *Adv. Prot. Chem.* **39**, 51–124.
5. Kirby, A.J. (1994) Enzyme mimics. *Angew. Chem. Int. Ed. Engl.* **33**, 551–553.
6. Ibers, J.A. & Holm, R.H. (1980) Modeling coordination sites in metallobiomolecules. *Science* **209**, 223–235.
7. Scarpa, M., Vianello, F., Signor, L., Zennaro, L. & Rigo, A. (1996) Ascorbate oxidation catalyzed by bis (histidine) copper (II). *Inorg. Chem.* **35**, 5201–5206.
8. Fields, G.B. & Noble, R.L. (1990) Solid phase peptide synthesis utilizing 9-fluorenylmethoxycarbonyl amino acids. *Int. J. Peptide Prot. Res.* **35**, 161–214.
9. Knorr, R., Trzeciak, A., Bannwarth, W. & Gillessen, D. (1989) New coupling reagents in peptide chemistry. *Tetrahedron Lett.* **30**, 1927–1930.
10. Braunschweiler, L. & Ernst, R.R. (1983) Coherence transfer by isotropic mixing: application to proton correlation spectroscopy. *J. Magn. Reson.* **53**, 521–528.
11. Wüthrich, K. (1986) *NMR of Proteins and Nucleic Acids*. J. Wiley & Sons, New York.
12. Weiner, S.J., Kolmann, P.A., Case, D.A. *et al.* (1984) Force field for simulation of proteins. *J. Am. Chem. Soc.* **106**, 765–784.
13. Rigo, A. & Rotilio, G. (1977) Simultaneous determination of superoxide dismutase and catalase in biological materials by polarography. *Anal. Biochem.* **81**, 157–166.
14. Fridovich, I. (1985) Cytochrome c. In *CRC Handbook of Methods for Oxygen Radical Research* (Greenwald, R.A., ed.). CRC Press, Boca Baton pp. 121–122.
15. Martin, B. (1979) Complexes of α-amino acids with chelatable side chain donor atoms. In *Metal Ions in Biological Systems* Vol. 9 (Siegel, H., ed.). Marcel Dekker Inc, New York pp. 1–39.
16. Glusker, J. (1991) Structural aspects of metal liganding to functional groups in proteins. *Adv. Prot. Chem.* **42**, 1–76.
17. Tainer, J.A., Getzoff, E.D., Beem, K.M., Richardson, J.S. & Richardson, D.C. (1982) Determination and analysis of the 2 Å structure of Cu, Zn superoxide dismutase. *J. Biol. Mol.* **160**, 181–217.
18. Masserschmidt, A., Rossi, A., Ladenstein, R. *et al.* (1989) Refined crystal structure of ascorbate oxidase at 1.9 Å resolution. *J. Mol. Biol.* **206**, 513–529.
19. Volbeda, A. & Hol, W. G. J. (1989) Pseudo 2-fold symmetry in the copper-binding domain of arthropodan haemocyanins. *J. Mol. Biol.* **209**, 249–279.
20. Bode, W., Gomis-Rüth, F.X., Huber, R., Zwilling, R. & Stöcker, W. (1992) Structure of astacin and implications for activation of astacins and zinc-ligation of collagenases. *Nature* **358**, 164–167.
21. Regan, L. (1995) Protein design: novel metal-binding sites. *Trends. Biochem. Sci.* **20**, 280–285.
22. Berg, J.M. (1988) Proposed structure for the zinc-binding domains from transcription factor IIIA and related proteins. *Proc. Natl. Acad. Sci. USA* **85**, 99–102.
23. Todd, R., Van Dam, M.E., Casimiro, D., Haymore, B.L. & Arnold, F.H. (1991) Cu (II) binding properties of a cytochrome c with a synthetic metal-binding site: $His\text{-}X_3$-His in an α-Helix. *Proteins: Struct. Funct. Gen.* **10**, 156–161.
24. Balakrishnan, R., Parthasarathy, R. & Sulkowski, E. (1998) Alzheimer's beta-amyloid peptide: affinity for metal chelates. *J. Pept. Res.* **51**, 91–95.
25. Argese, E., Viglino, P., Rotilio, G., Scarpa, M. & Rigo, A. (1987) Electrostatic control of the rate-determining step of the copper, zinc superoxide dismutase catalytic reaction. *Biochemistry* **26**, 3224–3228.
26. Stevanato, R., Mondovi', B., Befani, O., Scarpa, M. & Rigo, A. (1994) Electrostatic control of oxidative deamination catalysed by bovine serum amine oxidase. *Biochem. J.* **299**, 317–320.
27. Marqusee, S. & Baldwin, R. (1987) Helix stabilization by $Glu^-...Lys^+$ salt bridges in short peptides of *de novo* design. *Proc. Natl. Acad. Sci. USA* **84**, 8898–8902.

28. Shoemaker, K.R., Kim, P.S., York, E.J., Stewart, J.M. & Baldwin, R.L. (1987) Tests of the helix dipole model for stabilization of alpha-helices. *Nature* **326**, 563–567.
29. Espersen, G.W. & Martin, R.B. (1976) Predominant scalar interactions in selective broadening of ligand nuclear magnetic resonances by copper (II) ions. *J. Am. Chem. Soc.* **98**, 40–44.
30. Rigo, A., Viglino, P., Argese, E., Terenzi, M. & Rotilio, G. (1979). Nuclear magnetic relaxation of fluorine-19 as a novel assay method of superoxide dismutase. *J. Biol. Chem.* **254**, 1759–1760.
31. Vianello, F., Di Paolo, M.L., Zennaro, L., Stevanato, R. & Rigo, A. (1992) Isolation of amine oxidase from bovine plasma by two-step procedure. *Prot. Exp. Purif.* **3**, 362–367.
32. Bertini, I. & Luchinat, C. (1986) *NMR of Paramagnetic Molecules in Biological Systems.* Benjamin/Cummings, Menlo Park, CA, USA, pp. 47–101.
33. Dwek, R.A. (1973) *Nuclear Magnetic Resonance in Biochemistry*. Clarendon Press, Oxford, pp. 39–45.
34. Charlot, G. (1974) *Chimie Analytique Quantitative*, Vol. II. Masson, Paris, pp. 30–31.
35. Fee, J.A. & Ward, R.L. (1976) Evidence for a coordination position available to solute molecules on one of the metals at the active center of reduced bovine superoxide dismuatse. *Biochem. Biophys. Res. Commun.* **71**, 427–437.
36. Brill, A.S., Martin, R.B. & Williams, R. J. P. (1964) Copper in biological systems. In *Electronic Aspects of Biochemistry* (Pulmann, B., ed.). Academic Press, New York pp. 519–557
37. Butler, J.N. (1964) *Ionic Equilibrium.* Addison Wesley, Reading.
38. Sundberg, R.J. & Martin, R.B. (1974) Interactions of histidine and other imidazole derivatives with transition metal ions in chemical and biological systems. *Chem. Rev.* **74**, 471–515.
39. Peisach, J. & Blumberg, W. (1974) Structural implications derived from the analysis of electron paramagnetic resonance spectra of natural and artificial copper proteins. *Arch. Biochem. Biophys.* **165**, 691–708.
40. Aiba, H., Yokoyama, A. & Tanaka, H. (1974) Copper (II) complexing of Glycyl-L-histidine, Glycyl-L-histidylglycine, and Glycylglycyl-L-histidine in aqueous solution. *Bull. Chem. Soc. Jpn.* **47**, 1437–1441.
41. Wiesemann, F., Teipel, S., Krebs, B. & Hoeweler, U. (1994) Force field calculations on the structures of transition metal complexes. 1. Application to copper (II) complexes in square-planar coordination. *Inorg. Chem.* **33**, 1891–1898.
42. Sabolovic, J. & Rasmussen, K. (1995) *In vacuo* and in crystal molecular-mechanical modeling of copper (II) complexes with amino acids. *Inorg. Chem.* **34**, 1221–1232.
43. Martell, A.E. (1982) Chelates of ascorbic acid. Formation and catalytic properties. In *Ascorbic Acid: Chemistry, Metabolism and Uses* (Seib, P. & Tolbert, B., eds.), Adv. Chem. Ser. 200. American Chemical Society, Washington DC, pp. 153–178
44. Scarpa, M., Stevanato, R., Viglino, P. & Rigo, A. (1983) Superoxide ion as active intermediate in the autoxidation of ascorbate by molecular oxygen. *J. Biol. Chem.* **258**, 6695–6697.
45. Laroff, G.P., Fessenden, R.W. & Schuler, R.H. (1972) The electron spin resonance spectra of radical intermediates in the oxidation of ascorbic acid and related substances. *J. Am. Chem. Soc.* **94**, 9062–9073.
46. Kimura, E., Sakomnaka, A. & Nakamoto, M. (1981) Superoxide dismutase activity of macrocyclic polyamine complexes. *Biochim. Biophys. Acta* **678**, 172–179.
47. Goldstein, S., Czapski, G. & Meyerstein, D. (1990) A mechanistic study of the copper (II) - peptide-catalyzed superoxide dismutation. A pulse radiolysis study. *J. Am. Chem. Soc.* **112**, 6489–6492.
48. Amar, C., Vilkans, E. & Foos, J. (1982) Catalytic activity studies of some copper (II) - histidine-containing dipeptide complexes on aqueous superoxide ion dismutation. *J. Inorg. Biochem.* **17**, 313.
49. Dawson, R., Elliott, D., Elliott, W. & Jones, K. (1984) Amino acids, amines, amides, peptides and their derivatives. In *Data for Biochemical Research*. Clarendon Press, Oxford, pp. 1–31.
50. Kruck, T. & Sarkar, B. (1973) Structure of the species in the copper (II)-L-histidine system. *Can. J. Chem.* **51**, 3563–3571.
51. Butler, J., Koppenol, W.H. & Margoliash, E. (1982) Kinetics and mechanism of the reduction of ferricytochrome c by superoxide anion. *J. Biol. Chem.* **257**, 10747–10750.